Analyzing the Tensile Behavior of Warp-Knitted Fabric Reinforced Composites
Part I: Modeling the Geometry of Reinforcement

Hadi Dabiryan and Ali Asghar Asgharian Jeddi

***Abstract*— Fabrics have been increasingly used as reinforcement of composites. Due to the key role of the reinforcement in the mechanical properties of composites, the structure of warp-knitted fabrics is considered as the first part of a series of studies. Queen's cord structure is widely used in composite materials because of high stability. Therefore, the structure of Queen's cord fabrics has been analyzed as reinforcement of warp-knitted reinforced composites. For this purpose, a straight line model has been developed to fulfill the geometry of this kind of fabrics. To verify the generated model, Queen's cord fabrics in three densities were produced. Dimensional properties i.e. weight per unit area, front bar run-in, back bar run-in and total run-in of the produced fabrics were measured and compared with that of the model. The results showed that straight line model is capable of predicting the dimensional properties of this fabric.**

Keywords: **composite, Queen's cord, tensile behavior, warp-knitted fabric**

Nomenclature

Symbol	Quantity
l_{1f}, l_{2f}, l_{3f}	Length of segment of head of front bar loop
l_{1b}, l_{2b}, l_{3b}	Length of segment of head of back bar loop
l_{a1f}, l_{a2f}	Length of arms in front bar loop
l_{a1b}, l_{a2b}	Length of arms in back bar loop
l_{rf}	Length of roots in front bar
l_{rb}	Length of roots in back bar
l_{uf}	Length of front bar underlap
l_{ub}	Length of back bar underlap
n_b	Number of underlaps for the back bar
FB	Front bar
d	Yarn diameter
A	Yarn cross-section area
α_f,β_f	Angles of front bar legs in plane
α_b,β_b	Angles of back bar legs in plane
Φ_{1f},Φ_{2f},Φ_{3f}	Angles of front bar legs out of plane
Φ_{1b},Φ_{2b},Φ_{3b}	Angles of back bar legs out of plane
w	Wale spacing
c	Course spacing
BB	Back bar

H. Dabiryan and Ali. A. A. Jeddi are with the Department of Textile Engineering, Amirkabir University of Technology, Tehran, Iran. Correspondence should be addressed to H. Dabiryan (e-mail: dabiryan@aut.ac.ir).

I. Introduction

Composite materials have numerous advantages in comparison with conventional engineering metals. During recent years, textile composites have been widely used in different industries because of their high stiffness to weight ratio, good impact resistance, and good durability. These superior properties are concerned with unique characteristics of textiles applied as reinforcement of composites. The increasing use of composite materials has spurred the researchers to develop theoretical models to predict their mechanical properties. Modeling the mechanical properties of textile composites is performed in two directions: continuum approach and micromechanical approach. In the continuum approach, the composite is considered as a homogeneous material having a uniform property, ignoring the property difference between each constituent [1]. In micromechanical modeling, a repeating unit cell (RUC) of composite is analyzed, and the derived equations are extended to the whole structure.

Advances occurred in the technology of machinery enable us to produce high performance fabrics in order to use in different industries. Various types of fabrics, i.e. woven, weft- and warp-knitted fabrics are used as reinforcement of composites for different applications. Knitted fabrics have high potential to produce advanced composites due to their complex structure. Varying knit parameters such as underlap, loop length and stitch density can influence the mechanical properties of composites. Also, knitted structures have exceptional formability due to their low resistance to deformation. In addition, some techniques such as warp-insertion, weft-insert and diagonal yarns in the structure of the warp knitted fabrics improve the mechanical properties of reinforced composites. Many attempts [2-9] have been done to investigate the mechanics of fabric reinforced composites. Most of the mentioned attempts concentrate on woven reinforced composites, but knitted reinforced composites have received little attention. Studies [6] showed that although knitted reinforced composites are inferior in terms of some mechanical properties such as in-plane strength and stiffness, they are generally superior in terms of energy absorption, bearing and notched strength, and fracture toughness. These types of composites are widely used in aircraft applications due to good bearing, tailorability for balanced in-plane properties, and highly automated fabrication process [8]. Wu *et al.* [9] investigated the mechanical properties of

warp-knitted reinforced composites, experimentally. They found that knitted structures greatly affect the in-plane anisotropic nature, the tensile strength, and the modulus of warp-knitted reinforced composites. Also, they suggested two fracture modes: a fracture that occurs at the extreme low volume fraction region in the course direction, and a fracture that occurs due to stress concentration at the loop interlocking region in the wale direction. Huysmans *et al.* [10] presented a progressive damage model for the prediction of the nonlinear tensile behavior of knitted fabric composites.

Most of the warp-knitted fabrics which are used in composite manufacturing have chain stitch, inserted weft and/or warp in their structures. Chain stitch and inserted yarns enhance the tensile modulus of reinforcement, and the anisotropy of a knitted composite can also be manipulated to suit a particular requirement. Queen's cord is one of the basic warp-knitted structures which have chain stitch lapping movement in the front guide bar. The dimension of the Queen's cord fabric changes very slightly in width. It gives a superior stability to this type of fabrics.

In this series of articles, it is tried to present a micromechanical model to investigate the tensile properties of warp-knitted reinforced composites. For this purpose, a geometrical model is presented for Queen's cord structure as the first part of this series. In our previous research a straight line model was presented to predict the dimensional parameters of two-guide-bar warp knitted fabrics [11]. In the presented model, it was assumed that all segments of the loops in the unit cell are straight lines. Based on the presented model, some dimensional parameters such as run-in and weight per unit area were calculated theoretically and compared with experimental results. Acceptable agreement between theoretical and experimental results showed that the straight line model can be applied to predict the dimensional parameters of warp knitted fabrics. Hence, in this study, it is tried to present a straight line model for Queen's cord structures for analyzing the mechanical behavior of warp-knitted reinforced composites.

II. Theory

It is well known that warp knitting is characterized by loop forming through the feeding of the warp yarns, usually from warp beams, parallel to the direction in which the fabric is produced. In warp knitting technology, a series of yarns is knitted using the movement of guide bars relative to the needles. The pattern of fabrics is related to the lapping movement of guide bars. There are three types of movements on the guide bar, namely

- forward and backward swing;
- lateral movement for overlaps; and
- lateral movement for underlaps.

The first one is controlled by the cam shaft, the next two are controlled by the chain links.

The lapping movement of Queen's cord fabrics is illustrated in Fig. 1 and the chain notations are:

- Front bar: 1-0/0-1
- Back bar: 3-2/1-0

It is possible to produce queen's cord fabrics with longer underlaps.

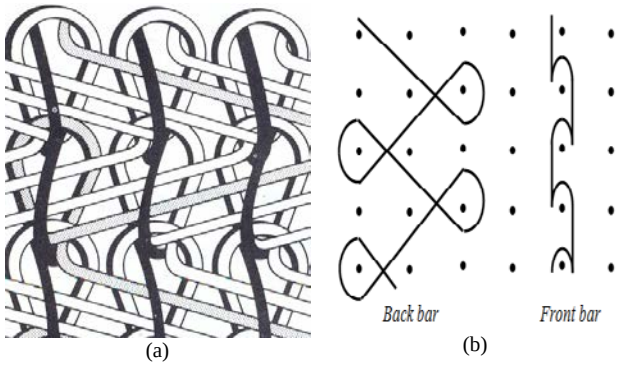

(a) (b)

Fig. 1. Queen's cord structure: a) Schematic of loops, b) lapping movements.

Fig. 2 shows the real photos of queen's cord structures. As it can be seen, a deviation from the wale direction has occurred in loops' position through the courses due to asymmetric structure of front and back bar loops. Based on the real photos, we can make the following assumptions for generating the straight line model:

- The yarn cross section is circle.
- All segments in loop structure are straight lines.
- The empty space in the head of loop is equal to the yarn diameters (Fig. 3).

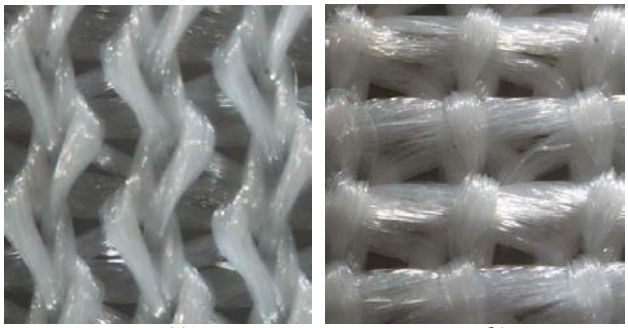

(a) (b)

Fig. 2. Queen's cord photos: a) front of fabric, b) back of fabric.

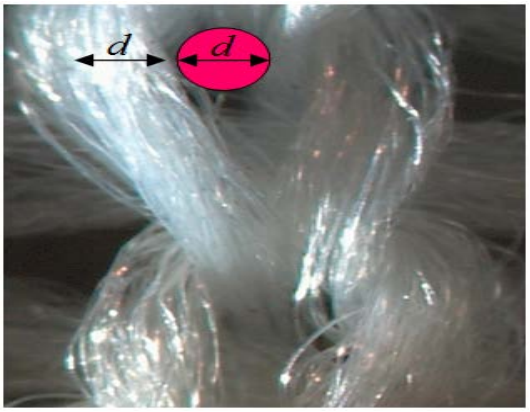

Fig. 3. The empty space in the loop structure.

Considering the deviation of loops, the schematic drawing shown in Fig. 4 can be proposed for modeling the geometry of Queen's cord structures. The suggested geometry demonstrates the skew of loops due to resultant of forces. Based on this geometry, front and back bar loops of Queen's cord structure are as the schematic drawing shown in Fig. 5.

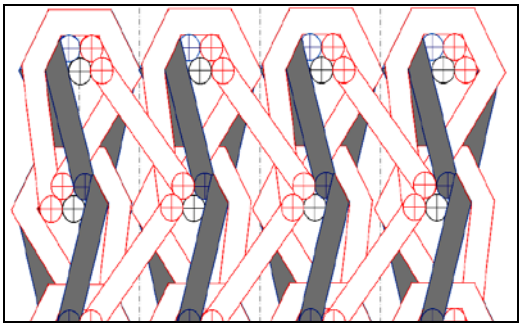

Fig. 4. A schematic of Queen's cord structures.

(a)

(b)

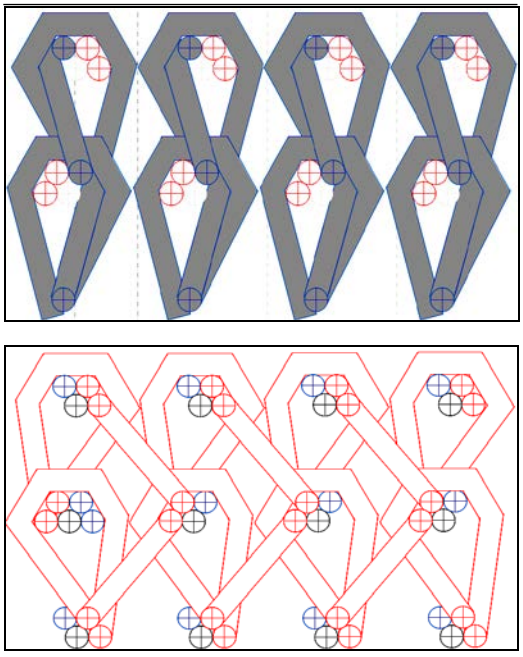

Fig. 5. Straight line model of Queen's cord structure: a) front bar loop, b) back bar loop.

In order to investigate the dimensional properties of the unit-cell, the loop length should be calculated first of all. For this purpose, we divide the unit-cell into two main parts: front bar loop and back bar loop. In this case, we can say the length of the unit-cell (L) is equal to:

$$L = L_f + L_b \tag{1}$$

where L_f and L_b are the length of the front and back bar loops, respectively.

As was pointed out, the main difference between structures with chain stitch loop and other common structures is the deviation of loop direction from the wale alignment, which should be considered in the dimensional properties of fabrics. Since, this deviation is due to the chain stitch movement in the front bar, the structure of front bar loop is treated, and the amount of the deviation is obtained as the preliminary stage of geometrical calculations. This value can be used for dimensional calculation of both front and back bars. According to Fig. 6, the deviation is equal to $Q"Q'$. By considering the geometrical relationship, the length of $Q"Q'$ can be calculated as bellow (See Appendix I):

$$Dev. = Q"Q' = 1.5d - tan\gamma.\left(c - \frac{\sqrt{3}}{2}.d\right) \tag{2}$$

where,

$$\gamma = \tan^{-1}\left(\frac{1.5d}{2c - \frac{\sqrt{3}}{2}.d}\right) + sin^{-1}\left(\frac{d}{\sqrt{2.25d^2 + \left(2c - \frac{\sqrt{3}}{2}.d\right)^2}}\right)$$

A. Front Bar Loop Calculations

As it can be seen in Fig. 6, the unit-cell of front bar should be investigated in two courses. According to this figure, the length of the front bar is obtained as follows:

$$L_f = l_{1f} + l_{2f} + l_{3f} + l_{a1f} + l_{a2f} + l_{uf} + l_{rf} \tag{3}$$

It should be noted that the root section (l_{rf}) cannot be seen in 2D model.

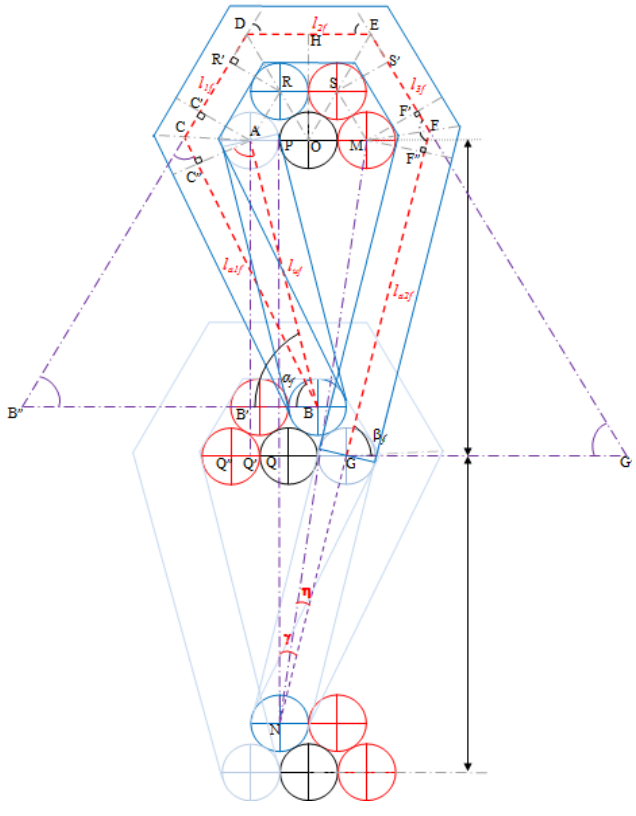

Fig. 6. Geometrical details of the front bar.

Considering the straight line model and the geometrical relationship, the length of different sections can be calculated using these equations:

$$l_{1f} = \frac{d}{\tan\left(\frac{\alpha_f}{2}+\frac{\pi}{6}\right)} + d + \frac{d}{\sqrt{3}} \quad (4)$$

$$l_{2f} = 2.15d \quad (5)$$

$$l_{3f} = \frac{d}{\sqrt{3}} + d + \frac{d}{\tan\left(\frac{\beta_f}{2}+\frac{\pi}{6}\right)} \quad (6)$$

$$l_{uf} = \sqrt{\left(tan\gamma.\left(c-\frac{\sqrt{3}}{2}.d\right)\right)^2 + (c-\frac{\sqrt{3}}{2}.d)^2} \quad (7)$$

$$l_{a1f} = \sqrt{{l_{uf}}^2 - d^2} + \frac{\mathrm{d}}{\tan\left(\frac{\alpha_f}{2}+\frac{\pi}{6}\right)} \quad (8)$$

$$l_{a2f} = \frac{d}{\tan\left(\frac{\beta_f}{2}+\frac{\pi}{6}\right)} + \frac{d}{\tan\eta} - \frac{\left(c-\frac{\sqrt{3}}{2}.d\right)}{Cos\gamma} \quad (9)$$

$$l_{rf} = 2d \quad (10)$$

$$\alpha_f = \sin^{-1}\left(\frac{c-\frac{\sqrt{3}}{2}.d}{l_{uf}}\right) - \sin^{-1}\left(\frac{d}{l_{uf}}\right) \quad (11)$$

$$\beta_f = \frac{\pi}{2} - \gamma \quad (12)$$

$$\eta = sin^{-1}\left(\frac{d}{\sqrt{2.25d^2+\left(2c-\frac{\sqrt{3}}{2}.d\right)^2}}\right) \quad (13)$$

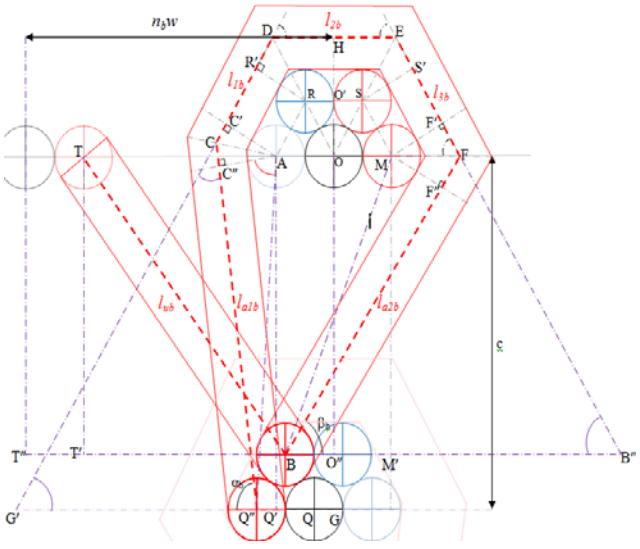

Fig. 7. Straight line model for back bar loop.

B. Back Bar Loop Calculations

A schematic of the generated model for back bar loop is shown in Fig. 4(b). Based on this model, the details of back bar loop are as in Fig. 7. It is well known that the length of the back bar loop (L_b) is equal to:

$$L_b = l_{1b} + l_{2b} + l_{3b} + l_{a1b} + l_{a2b} + l_{ub} + l_{rb} \quad (14)$$

Using geometrical relationships, it can be shown that the length of different sections is calculated as follows:

$$l_{1b} = \frac{d}{\tan\left(\frac{\alpha_b}{2}+\frac{\pi}{6}\right)} + d + \frac{d}{\sqrt{3}} \quad (15)$$

$$l_{2b} = 2.15d \quad (16)$$

$$l_{3b} = \frac{d}{\sqrt{3}} + d + \frac{d}{\tan\left(\frac{\beta_b}{2}+\frac{\pi}{6}\right)} \quad (17)$$

$$l_{ub} = \sqrt{(c-\frac{\sqrt{3}}{2}.d)^2 + [n_b w - 1.5d - Dev.]^2} \quad (18)$$

$$l_{a1b} = \sqrt{c^2 + dev.^2 - d^2} + \frac{d}{\tan\left(\frac{\alpha_b}{2}+\frac{\pi}{6}\right)} \quad (19)$$

$$l_{a2b} = \sqrt{\left(c-\frac{\sqrt{3}}{2}.d\right)^2 + (1.5\mathrm{d} + Dev.)^2 - d^2} + \frac{d}{\tan\left(\frac{\beta_b}{2}+\frac{\pi}{6}\right)} \quad (20)$$

$$l_{rb} = \frac{\sqrt{3}}{2}d \quad (21)$$

$$\alpha_b = \pi - \sin^{-1}\left(\frac{d}{\sqrt{c^2+Dev.^2}}\right) - \tan^{-1}\left(\frac{c}{Dev.}\right) \quad (22)$$

$$\beta_b = \tan^{-1}\left(\frac{c-\frac{\sqrt{3}}{2}.d}{1.5d+Dev.}\right) - \sin^{-1}\left(\frac{d}{\sqrt{(c-\frac{\sqrt{3}}{2}.d)^2+(1.5d+Dev.)^2}}\right) \quad (23)$$

The model of back bar can be extended to other structures by increasing the number of back bar underlaps (n_b). For example, the number of underlaps in the fabrics considered in this study is 2, so in our calculations we have: n_b=2.

C. 3D State of the Model

Due to the 3D nature of knitted fabrics, we should calculate the length of all sections in 3D state. A straight line model has been proposed for side view of unit-cell which shows the loops in 3 dimensions (Fig. 8).

As it can be seen in 3D model, some sections such as l_{1f}, l_{1b}, l_{a2f} and l_{a2b} make angles Φ_{1f}, Φ_{1b}, Φ_{2f} and Φ_{2b} with the longitudinal direction, respectively. Therefore, their lengths should be calculated in 3D state. For this purpose, we need to obtain aforementioned angles which can be calculated as bellow:

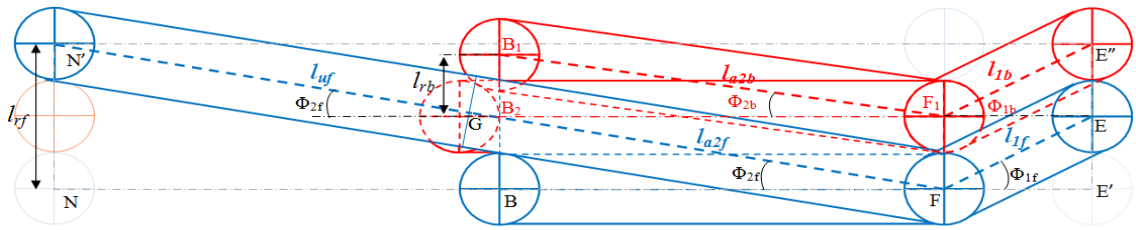

Fig. 8. Straight line model for side view of the unit-cell.

$$\Phi_{1f} = \tan^{-1}\left(\frac{d}{\frac{d}{\tan\left(\frac{\alpha_f}{2}+\frac{\pi}{6}\right)}+\frac{(1+\sqrt{3})d}{\sqrt{3}}}\right) \quad (24)$$

$$\Phi_{1b} = \tan^{-1}\left(\frac{d}{\frac{d}{\tan\left(\frac{\alpha_b}{2}+\frac{\pi}{6}\right)}+\frac{(1+\sqrt{3})d}{\sqrt{3}}}\right) \quad (25)$$

$$\Phi_{2f} = \tan^{-1}\left(\frac{2d}{\sqrt{\left(\left(2c-\frac{\sqrt{3}}{2}.d\right)^2+1.25d^2\right)}+\frac{d}{\tan\left(\frac{\beta}{2}+\frac{\pi}{6}\right)}}\right) \quad (26)$$

$$\Phi_{2b} = \sin^{-1}\left(\frac{\frac{\sqrt{3}}{2}d}{\frac{d}{\tan\left(\frac{\beta_b}{2}+\frac{\pi}{6}\right)}+\sqrt{\left(c-\frac{\sqrt{3}}{2}.d\right)^2+(1.5\mathrm{d}+Dev.)^2-d^2}}\right) \quad (27)$$

Referring to the suggested 3D model (Fig. 8), it can be seen that the angles which l_{3f} and l_{3b} make with the fabric plane are equal to the angels that l_{1f} and l_{1b} make with that plane. So, we can write:

$$\Phi_{3f} = \Phi_{1f}$$
$$\Phi_{3b} = \Phi_{1b}$$

Thereafter, Eqs. (3) and (14) are modified for 3D state as bellow:

$$L_f = \frac{l_{1f}}{Cos\Phi_{1f}} + l_{2f} + \frac{l_{3f}}{Cos\Phi_{3f}} + l_{a1f} + \frac{l_{a2f}}{Cos\Phi_{2f}} + \frac{l_{uf}}{Cos\Phi_{2f}} + l_{rf} \quad (28)$$

$$L_b = \frac{l_{1b}}{Cos\Phi_{1b}} + l_{2b} + \frac{l_{3b}}{Cos\Phi_{3b}} + l_{a1b} + \frac{l_{a2b}}{Cos\Phi_{2b}} + l_{ub} + l_{rb} \quad (29)$$

Based on the above equations, the front bar run-in (R_f) and the back bar run-in (R_b) are obtained as follows:

$$R_f = 480L_f \quad (30)$$

$$R_b = 480L_b \quad (31)$$

$$R_t = R_f + R_b \quad (32)$$

Also, we can use Eq. (33) to calculate the theoretical weight per unit area:

TABLE I
CHARACTERISTICS OF PRODUCED FABRICS

Fabric structure	density	Fabric code	Number of underlaps		Run-in (*cm/rack**)		CPC	WPC	Fabric mass (g m^{-2})
			FB	BB	FB	BB			
Queen's Cord	loose	*Q2l*	1	2	154	223	12.6	11.9	98.12
	medium	*Q2m*	1	2	124	180	19.4	12.1	126.1
	tight	*Q2t*	1	2	117	171	23.3	11.8	137.5
Queen's Cord	loose	*Q3l*	1	3	155	281	12.1	11.6	106.3
	medium	*Q3m*	1	3	129	234	17.3	11.8	128.6
	tight	*Q3t*	1	3	112	204	22.9	11.6	146
Queen's Cord	loose	*Q4l*	1	4	152	331	11.8	11.8	116.6
	medium	*Q4m*	1	4	128	280	17.4	11.8	145.6
	tight	*Q4t*	1	4	110	240	22.8	11.8	163.6

$$W[\frac{g}{m^2}] = \frac{wpc \times cpc \times R_t \times den}{480 \times 90} \quad (33)$$

III. Verification of the Model

To evaluate the accuracy of the generated model, Queen's cord fabrics were produced in three different densities using 75 denier (8.3 tex)/36 filament polyester yarn. A positive let-off system, 28-gauge warp-knitting machine was used. The structural details of the fabrics are given in Table I. The fabric samples were then left at room atmosphere (25°C $\pm$1 & 30%$\pm$3 RH) for some days before being washed for 30 minutes at a temperature of 30°C in a Winch washing machine with a detergent. Then, the fabrics were relaxed on a flat surface and left to condition over night at the same room atmosphere.

The theoretical results of dimensional properties are presented in Table II.

TABLE II
Theoretical Results of Dimensional Parameters

Fabric code	Run-in (*cm/rack**)			Fabric mass (g m^{-2})
	Front bar	Back bar	Total	
Q2l	155	192	347	90
Q2m	118	162	279	114
Q2t	107	155	262	125
Q3l	159	237	396	96
Q3m	126	209	335	119
Q3t	108	198	306	141
Q4l	162	276	438	106
Q4m	125	249	374	133
Q4t	108	237	345	161

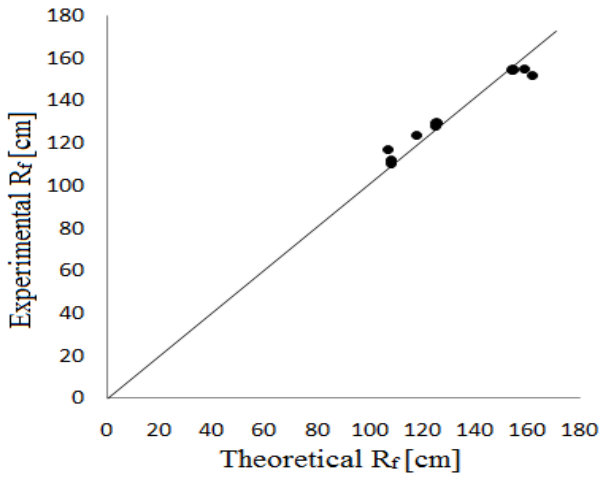

Fig. 9. The comparison of theoretical and experimental values of front bar run-in.

The correlation between the theoretical and the experimental results of the front bar and back bar run-in are shown in Figs. 9 and 10, respectively. Fig. 9 demonstrates that there is a good agreement between experimental and theoretical values of front bar run-in, while the difference between those of back bar run-in is more significant (Fig. 10).

In Fig. 10 the experimental values are mostly more than the theoretical results. It is attributed to the difference between the curve shape of the yarn segments in the real structure and the straight line shape of them in the generated model. In straight line model the real curve of the yarn segments is replaced by straight line. Therefore, the difference between the real and theoretical results is increased by increasing the yarn length in the unit-cell (Fig. 11).

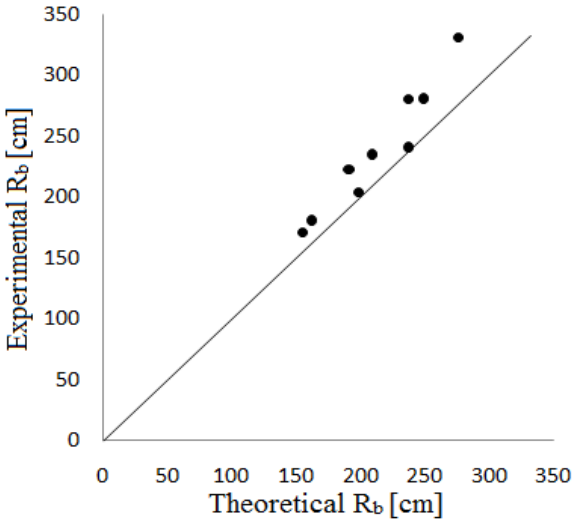

Fig. 10. The comparison of theoretical and experimental values of back bar run-in.

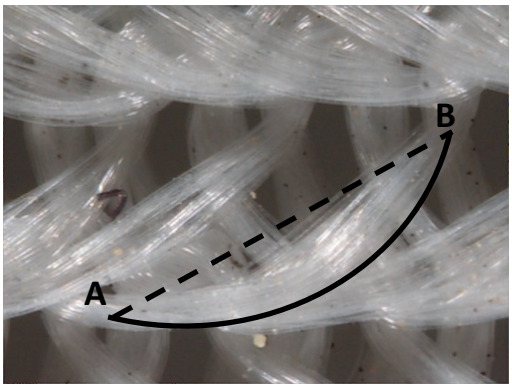

Fig. 11. The difference between real curves in the fabrics and straight lines in the model.

In Fig. 12 the experimental and theoretical values of total run-in of the fabric are compared. The correlation shown between the results confirm that the generated model is capable of predicting the run-in of fabrics acceptably.

Fig. 13 shows the comparison between theoretical and experimental values of the weight per unit area of the fabrics. This figure demonstrates that the experimental values are slightly more than the theoretical values.

To be more precise, the mean error percentage for each parameter is shown in Table III. Based on the presented data in this table, we can say in most of the cases the

model can predict the dimensional parameters of fabrics, reasonably.

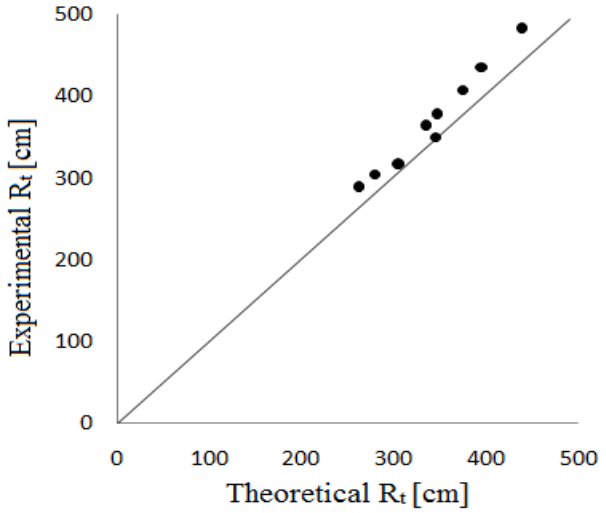

Fig. 12. The comparison of theoretical and experimental values of total run-in

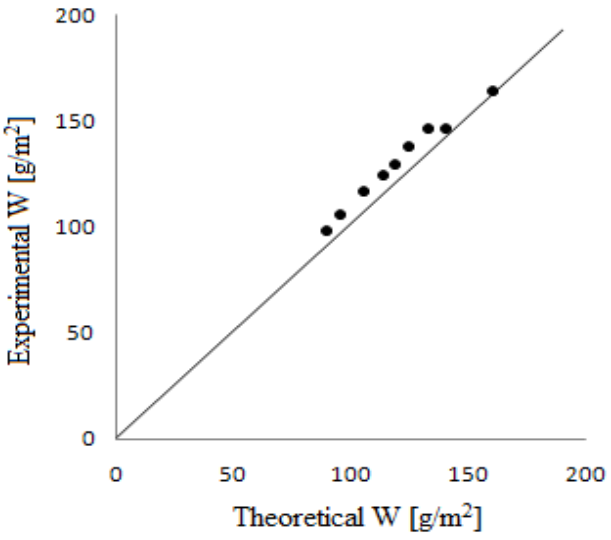

Fig. 13. The comparison of theoretical and experimental values of weight per unit area.

TABLE III
ERROR PERCENTAGE IN PREDICTION OF DIMENSIONAL PARAMETERS

Front Bar Run-in(%)	Back Bar Run-in(%)	Total Run-in (%)	Weight per Unit Area (%)
3.8	10.2	7.2	7.2

IV. CONCLUSION

It is noteworthy that reinforcements play a main role in the mechanical properties of composites. Therefore, in analyzing the mechanical properties of textile composites it is necessary to investigate the structure of fabrics. Tensile properties of warp-knitted reinforced composites considerably depend on the structure of warp knitted fabrics. Due to the wide application of Queen's cord structures in composite materials, this type of fabrics was chosen. For modeling the warp-knitted fabrics, we needed to make a simplification in their geometry because of their complex structure. Therefore, the geometry of Queen's cord fabrics was modeled using a straight line model. To evaluate the model, the dimensional parameters, i.e. weight per unit area, front bar, back bar and total run-in of produced fabrics were measured and compared with the theoretical results of the model. The results showed that the straight line model can predict the dimensional parameters of reinforcement.

REFERENCES

[1] J. H. Kim, M. G. Lee, H. Ryou, K. Chung, J. R. Youn, and T. J. Kang, "Development of Nonlinear Constitutive Laws for Anisotropic and Asymmetric Fiber Reinforced Composites", *Polym. composite*, vol. 22, no. 2, pp. 216-228, 2008.

[2] P. Xue, J. Cao, and J. Chen, "Integrated Micro/Macro-mechanical Model of Woven Fabric Composites under Large Deformation", *Compo. Struct.*, vol. 70, pp. 69–80, 2005.

[3] C. T. Key, S. C. Schumacher, and A. C. Hansen, "Progressive Failure Modeling of Woven Fabric Composite Materials using Multicontinuum theory", Composites: Part B,vol. 38, pp. 247–257, 2007.

[4] S. Song, A. M. Waas, K. W. Shahwan, and Xiao, "Braided Textile Composites under Compressive Loads: Modeling the Response, Strength and Degradation", *Compos. Sci. and Technol.*, vol. 67, pp. 3059–3070, 2007.

[5] Y. Miao, E. Zhou, Y. Wang, and B. A. Cheeseman, "Mechanics of Textile Composites: Micro-geometry", *Compos. Sci. and Technol.*, vol. 68, pp. 1671–1678, 2008.

[6] M. Li, S. Wang, Z. Zhang and B. Wu, "Effect of Structure on the Mechanical Behaviors of Three-Dimensional Spacer Fabric Composites", *Appl. Compos. Mater.*, vol.16, pp. 1–14, 2009.

[7] K. H. Leong, S. Ramakrishnab, Z. M. Huangb, G.A. Bibo, "The Potential of Knitting for Engineering Composites", *Composites: Part A*, Vol. 31, 197–220, 2000.

[8] H. B. Dexter, "Development of Textile Reinforced Composites for Aircraft Structures", 4th International Symposium for Textile Composites, Kyoto, Japan, Oct. 12th -14th, 1998.

[9] W. L. Wu, M. Kotaki, and A. Fujita, "Mechanical Properties of Warp-Knitted, Fabric-Reinforced Composites, *J. Reinf. Plast. Comp.*, vol. 12, pp. 1096-1110, 1993.

[10] G. Huysmans, I. Verpoest, and P. V. Houtte, "A Damage Model for Knitted Fabric Composites", *Composites: Part A*, vol. 32, pp. 1465-1475, 2001.

[11] H. Dabiryan, and Ali A. A. Jeddi, "Analysis of Warp Knitted Fabric Structure: Part I: A 3D Straight Line Model for Warp Knitted Fabrics", *J. Text. Inst.*, vol. 102, no. 12, pp. 1065-1074, 2011.